IJARSCT
ISSN (Online) 2581-9429
International Journal of Advanced Research in Science, Communication and Technology (IJARSCT)
Volume 7, Issue 2, July 2021
Impact Factor: 5.731

Rietveld Refinement and Study of Elastic Properties of $Ni_{0.7}Zn_{0.3}Dy_xFe_{2-x}O_4$ ($0.0 \leq x \leq 0.03$) Ferrite Nano-Structures

S. S. Kammar
Department of Physics
HKE's A. V. Patil Degree College, Aland, Kalburgi, Karnataka, India

Abstract: *Dy substituted spinel ferrite nanoparticles of the composition $Ni_{0.7}Zn_{0.3}Dy_xFe_{2-x}O_4$ (x = 0.0, 0.015, 0.03) were fabricated by using sol-gel method. Structural and elastic properties of Ni-Zn ferrite were tailored by introducing the Dy^{3+} rare earth ions. Powder X-ray diffraction (XRD) and Infrared spectroscopy (IR) techniques were employed to investigate the phase purity, absorption bands, and elastic properties of the samples. The crystal structure and cell parameters were refined by using Rietveld refinement done by using Fulprof software. Rietveld refinement infers that the ceramics crystallized in single – phase cubic spinel structure having the space group Fd-3m. A slight increase in lattice parameter is observed due to substitution of Dy^{3+} ions in Ni-Zn crystal lattice. The vibrational study was achieved by using IR spectroscopy. Two major absorption bands (υ_1 and υ_2) were observed in the frequency range of 350 to 800 cm^{-1} which confirms the co-existence of tetrahedral and octahedral sites of spinel structure. IR data was used to evaluate the elastic parameters like stiffness constant, young's modulus, bulk modulus, rigidity modulus, poisons ratio, and Debye temperature. All the elastic moduli and Debye temperature are found increasing with increasing concentration of Dy^{3+} ions.*

Keywords: X-ray diffraction, Rietveld refinement, infrared spectroscopy, elastic properties

I. INTRODUCTION

Ferrites are technologically important materials because of their unique properties like high coercivity, high permeability and very high resistivity and can be used in microwave and radio frequency devices [1-2]. The increasing trend in the fabrication of the modern technology has enhanced the performance of the devices from low to high frequency, better efficiency and miniaturization [3]. Ferrites are grouped in four categories such as cubic spinel, garnets, hexaferrites and magneto plumbites [4]. Spinel ferrites with cubic crystal geometry are belongs to the soft ferrites which have been the current topic of interest due to their excellent physico-chemical properties and versatile applications in various fields [5-6]. Spinel ferrites at nano-scale dimension shows some unique structural, chemical, physical, magnetic, dielectric properties and high frequency applications which are quite different from their bulk counterpart [7]. Such properties can be tailored by using different synthesis method, composition, amount and type of dopant and sintering conditions [8].

The electromagnetic properties of spinel ferrites are depending upon the Fe-Fe interactions, super exchange interactions of Me-Fe cations at lattice sites and spin coupling of 3d electrons. Moreover, substitution of rare earth ions in spinel lattice may enhanced the electromagnetic response of spinel ferrites [9]. The incorporation of RE ions into spinel lattice produces the RE-Fe (3d-4f coupling) interaction which in turn improves the electrical and magnetic properties of the spinel ferrites. Hence, in the recent years, study of RE doped spinel ferrites have been grown due to their extraordinary electromagnetic and optical properties [10-11]. Several reports are available on the study structural, elastic, electrical and magnetic properties of RE doped (e.g. Gd^{3+}, Sm^{3+}, Dy^{3+}, Ce^{3+}, Y^{3+}, Er^{3+}, Tb^{3+}, Pr^{3+}, Ho^{3+} etc.) spinel ferrites [12-15].

The increasing interest of scientific community towards RE doped spinel ferrites motivated us to study the effect of Dy^{3+} substitution in Ni-Zn spinel ferrites. In the present work nano-scale spinel ferrites having general chemical formula $Ni_{0.7}Zn_{0.3}Dy_xFe_{2-x}O_4$ (x = 0.0, 0.015, 0.03) have been synthesized by using sol-gel auto-combustion technique. As prepared samples were investigated by using X-ray diffraction technique (XRD) and infrared spectroscopy (IR) for the Rietveld refinement and study of elastic properties.

IJARSCT
ISSN (Online) 2581-9429
International Journal of Advanced Research in Science, Communication and Technology (IJARSCT)
Volume 7, Issue 2, July 2021
Impact Factor: 5.731

II. MATERIALS AND METHODS

Nickel nitrate ($Ni(NO_3)_2.6H_2O$), zinc nitrate ($Zn(NO_3)_2.6H_2O$), dysprosium nitrate ($Dy(NO_3)_3.9H_2O$), iron nitrate ($Fe(NO_3)_3.9H_2O$) were used as starting materials. The stoichiometric calculations of the raw materials were done by for the synthesis of Dy substituted Ni-Zn ferrites. For the gelation process, citric acid ($C_6H_8O_7.H_2O$) was also used as chelating agent. All the chemical were taken are highly pure (99.9%) and are of analytical grade.

To complete the gelation process, all the nitrates were act as oxidants and citric acid was act as fuel. All the nitrates and citric acid were liquified in deionized water with their stoichiometric weight proportion. The molarity ratio of nitrates and citric acid was taken as 1:3 in order to kept the stability of combustion process of nitrates from the solution. The beakers consisting nitrates and citric acid solution together were kept on magnetic stirrer with hot plate. The stirring was done for half an hour at toom temperature in order to get the clear and homogeneous solution of the nitrates. After that the solution was heated at constant temperature of 90^0C with continuous stirring. The pH of the mixture was maintained at 7 by adding the liquid ammonia dropwise. After 2-3 hours the solution gets converted into viscous sol and thereafter suddenly converted into dried gel. The dried gel after auto-ignition process with brown flint gets converted into fluffy brown ash. The ash was grinded for 2 hours and sintered at 800^0C for six hours. The dark brown powders after sintering were again grinded and converted into fine powders for further characterizations. The as prepared powders were characterized by using powder X-ray diffraction technique and infrared spectroscopy at room temperature. XRD data was collected in the 2θ range of 20^0 to 70^0 by using Phillips X-ray diffractometer (Model 3710). Cu-Kα radiations (λ=1.5406 Å) have been used and the scanning rate was maintained at 2^0 per minute. Infrared spectra were recorded by using Perkin Elmer within the frequency range of 350 to 800 cm^{-1}.

III. RESULTS AND DISCUSSION

Rietveld refined X-ray diffraction patterns of Dy^{3+} doped Ni-Zn nano-ferrites are shown in Fig. 1. The XRD patterns showed the fitted experimental and observed standard data with their difference and peak positions. It is observed that the Bragg's reflections of the XRD lines in experimental data is fitted very well with the observed data.

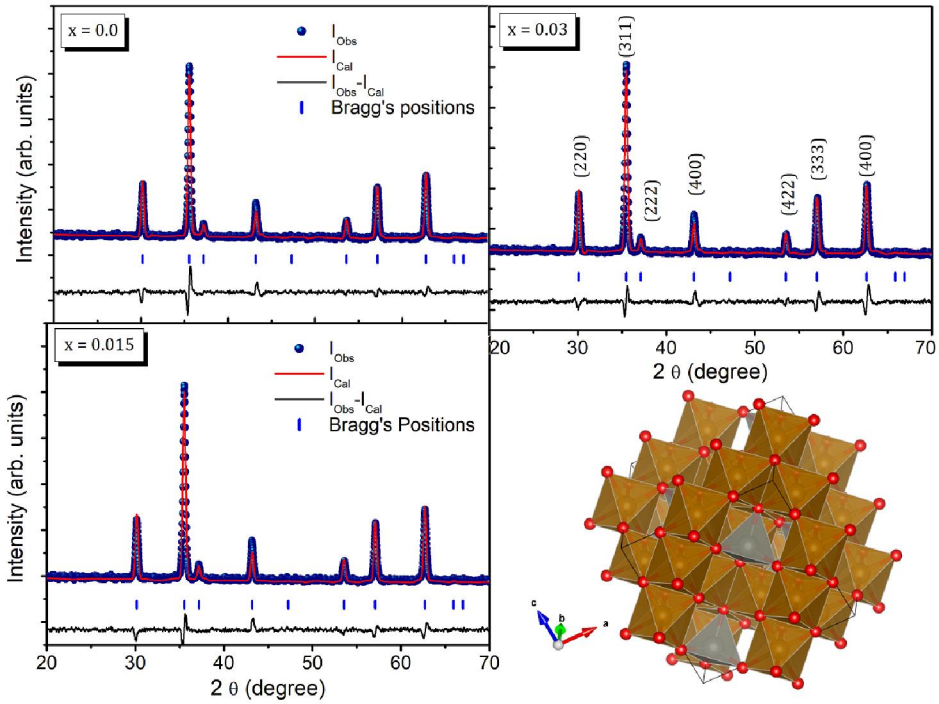

Fig. 1: Rietveld refined XRD patterns and crystal structure of $Ni_{0.7}Zn_{0.3}Dy_xFe_{2-x}O_4$

All the XRD patterns were analysed by using XpertHighScore Plus and Fullprof software's. To model the peak profile of the XRD lines based on Fd-3m space group, a Thompson -Cox-Hasting pseudo-Voigt function was used the oxygen

IJARSCT
ISSN (Online) 2581-9429
International Journal of Advanced Research in Science, Communication and Technology (IJARSCT)
Volume 7, Issue 2, July 2021
Impact Factor: 5.731

parameters (x=y=z=u) taken as free parameters while all other atomic fractional positions were considered as being fixed. The performed pattern reproduces adequately all the observed reflections and gave practically an identical reliability factor. The Rietveld refined XRD patterns show the formation of single-phase cubic spinel structure of the samples. To characterize the quality of fit, various reliability factors (R-factors) with Bragg's contributions such as goodness factor (χ^2), profile factor (R_P), weighted profile factor (R_{WP}), and experimental factor (R_{EXP}) were obtained from Rietveld refinement and are tabulated in Table 1. Values of goodness factor χ^2 are obtained between 1 and 2 which implies the best fitting quality of the XRD data. As the evaluated parameters from refinement reaches to their minimum value, and the crystal structure is evaluated satisfactorily, it indicates the best fit to the experimental data [16]. The values of lattice parameter obtained from Rietveld refinement are ranges from 8.3677 to 8.3821 Å with Dy^{3+} substitution in Ni-Zn ferrites. This increment in lattice parameter can be explained on the basis of difference in ionic radii of constituent ions.

Table 1: Rietveld refined parameters of $Ni_{0.7}Zn_{0.3}Dy_xFe_{2-x}O_4$ nano-ferrites.

'x'	'a' (Å)	χ^2	R_P	R_{WP}	R_{EXP}
0.0	8.3677	1.05	36.4	18.0	17.51
0.015	8.3733	1.09	35.7	17.1	16.32
0.03	8.3821	1.14	37.3	16.8	15.77

As depicted in Fig. 2, infrared spectra of $Ni_{0.7}Zn_{0.3}Dy_xFe_{2-x}O_4$ nano-ferrites are drawn in the wavenumber range of 350 to 800 cm^{-1}. As a common feature of spinel ferrite, it shows two main absorption bands in the range of 350 to 800 cm^{-1}. The high frequency band (υ_1) is observed in the range 552 to 561 cm^{-1} and low frequency band (υ_2) is observed in the wavenumber range of 383 to 392 cm^{-1}. Both υ_1 and υ_2 are shifted towards higher frequency region with the addition of Dy^{3+} ions in the Ni-Zn nano-ferrites. The variation of band position with Dy^{3+} substitution is shown in Fig. 3 (a). The change in the band position is expected due to the difference in the metal ion-oxygen distances for the octahedral and tetrahedral complexes [17].

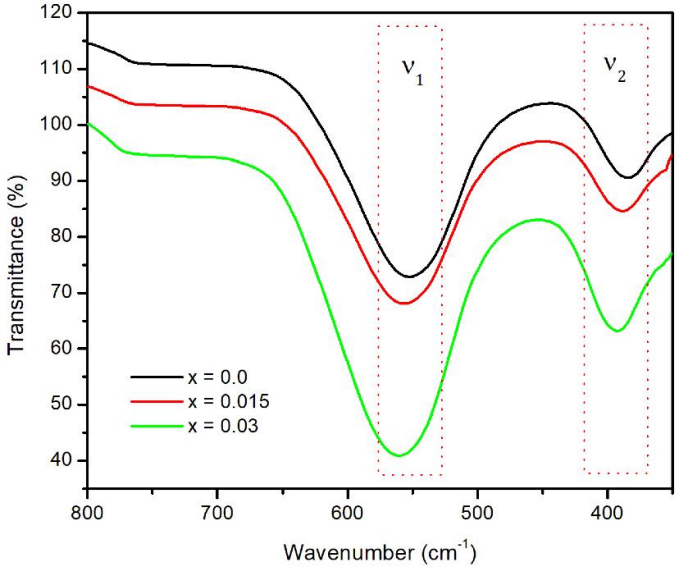

Fig. 2: Infrared spectra of $Ni_{0.7}Zn_{0.3}Dy_xFe_{2-x}O_4$

The force constants (K_t and K_O) are depending upon the ion distribution in the crystal lattice; with the help of Waldron's method the force constant can be calculated by using the following relations [18];

$$K_t = 7.62 \times M_A \times v_1^2 \ N/m \quad (1)$$

$$K_o = 10.62 \times M_B \times v_2^2 \ N/m \quad (2)$$

IJARSCT
ISSN (Online) 2581-9429
International Journal of Advanced Research in Science, Communication and Technology (IJARSCT)
Volume 7, Issue 2, July 2021
Impact Factor: 5.731

Where, υ_1 and $\upsilon_2$are the band positions in IR spectra, M_A and M_B are the molecular weights (Table 2) of corresponding sites. Variation of force constants with Dy^{3+} substitution is depicted in Fig. 3 (b).

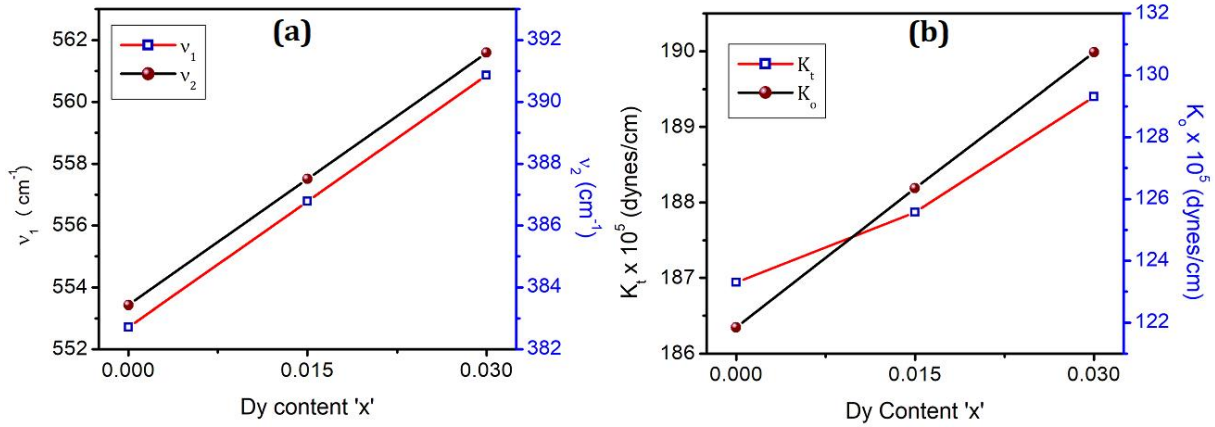

Fig. 3: (a) Variation of band positions (υ_1) and (υ_2) and (b) variation of force constants (K_t and K_o) with Dy content 'x' for $Ni_{0.7}Zn_{0.3}Dy_xFe_{2-x}O_4$

It can be seen form Fig. 3 (b) that force constant at tetrahedral site (K_t) is increases from 186.94 × 10^5 to 189.40 × 10^5dyens /cm and at octahedral site (K_o) it increases from 121.85 × 10^5 to 130.75 × 10^5 dynes/cm with the addition of Dy^{3+} ions. The Bulk modulus (B) of the spinel ferrites can be given by the equation [19];

$$B = \frac{1}{3}[C_{11} + 2C_{12}] \quad (3)$$

Where, C_{11} and C_{12} are the components of elasticity tensor, for isotropic materials with cubic spinel structure C_{11} is almost equal to C_{12} and hence B = C_{11}. Now the stiffness constant C_{11} can be obtained from the relation with K_{av} (≅ average of K_t and K_O) is $C_{11} = K_{av} / a$. Values of K_{av}, C_{11} and B are listed in Table 2.

Table 2: Elastic properties of $Ni_{0.7}Zn_{0.3}Dy_xFe_{2-x}O_4$.

'x'	0.0	0.015	0.03
M_A	80.31	79.53	79.02
M_B	156.08	158.46	160.57
K_{av} (×10^5 dynes/cm)	154.4	157.1	160.1
C_{11} (GPa)	184.54	187.62	190.99
V_l (m/s)	5866	5903	5944
V_t (m/s)	3387	3408	3432
B (GPa)	185	188	191
G (GPa)	61.51	62.54	63.66
σ	0.35	0.35	0.35
E (GPa)	166.09	168.86	171.89
V_m (m/s)	3760	3783	3810
θ_D (K) Anderson	673	679	685

IJARSCT
ISSN (Online) 2581-9429
International Journal of Advanced Research in Science, Communication and Technology (IJARSCT)
Volume 7, Issue 2, July 2021
Impact Factor: 5.731

Values of longitudinal wave velocity (V_L) and transverse wave velocity (V_T) are estimated by using following relations [18];

$$V_L = \sqrt{\frac{C_{11}}{dx}} \quad \text{and} \quad V_T = \frac{V_L}{\sqrt{3}} \tag{4}$$

Computed values of V_L and V_T are listed in Table 1 and are used to evaluate the rigidity modulus, poisons ratio, and Young's modulus by using following relations;

$$G = d_x V_T^2 \tag{5}$$

$$\sigma = \frac{(3B - 2G)}{(6B + 2G)} \tag{6}$$

$$E = (1 + \sigma)2G \tag{7}$$

All the results are listed in Table 2. A reason for the change of elastic moduli with Dy^{3+} concentration may be related to the change of inter-atomic bonding between various atoms. The Poisson's ratio remains constant at 0.35 for all the compositions. This value lies between the range of -1 to 0.5 which suggests the isotropic nature of the elasticity of the samples. The materials stability is due to the positive values of all elastic moduli.

Mean elastic wave velocity and Debye temperature are obtained by using the following relations;

$$V_m = \left[3\left\{ \frac{V_t^3 V_l^3}{V_t^3 + 2V_l^3} \right\} \right]^{1/3} \tag{8}$$

$$\theta_D = \left(\frac{h}{k_B} \right) \left(\frac{3N_A}{4\pi V_A} \right)^{1/3} V_m \tag{9}$$

Where, V_A is mean atomic volume which is given by $(Md_X)/q$, M is molecular weight, q is number of atoms in the formula unit, d_X is X-ray density, N_A is Avogadro's number, h is planks constant, and K_B is Boltzmann constant. Mean atomic volume (V_m) increases from 3760 to 2810 m/s and Debye's temperature increases from 673 to 685 K with the addition of Dy^{3+} ions in Ni-Zn crystal lattice.

II. CONCLUSION

Nanocrystalline ferrites powders of Dy^{3+} substituted Ni-Zn ferrites are prepared by using sol-gel route. Rietveld refined X-ray diffraction patterns confirms the cubic spinel structure of the samples with Fd-3m space group. Goodness factor obtained from refinement of XRD data lies between the range 1 to 2 which implies the better fitting quality of the data. Lattice constant obtained from Rietveld refinement increases from 8.3677 to 8.3821 Å with Dy^{3+} substitution. This increment in lattice constant can be explained on the basis of difference in ionic raidii of constituent ions. As a common feature of the spinel ferrites, IR spectra shows two major bands υ_1 and υ_2 lies between 350 to 800 cm^{-1}. All the elastic moduli show positive values which confirms the isotropic elasticity theory. Debye temperature increases from 673 to 685 K with the addition of Dy^{3+} ions in Ni-Zn crystal lattice.

REFERENCES

[1]. M. N. Akthar, M. Babar, S. Qmar, Z. Rehman, M. A. Khan; Structural Rietveld refinement and magnetic features of prosademium (Pr) doped Cu nanocrystalline spinel ferrites; Ceram. Inter. 45 (2019) 10187-10195

[2]. M. N. Akthar, A. A. Khan, M. N. Akhtar, M. Ahmed, M. A. Khan; Structural Rietveld refinement, morphological and magnetic features of Cu doped Co-Ce nanocrystalline ferrites for high frequency applications; Physica B: Cond. Matter. 561 (2019) 121-131.

[3]. V. D. More, S. R. Kadam, S. B. Shelke, P. D. Gaikwad, R. H. Kadam, S. T. Alone; Modified structural and magnetic properties of Ni-Mn-Zn ferrite nanoparticles doped with Ce^{3+} ions; Biointer. Res. Appl. Chem. 12 (2022) 5021-5030.

IJARSCT
ISSN (Online) 2581-9429
International Journal of Advanced Research in Science, Communication and Technology (IJARSCT)
Volume 7, Issue 2, July 2021
Impact Factor: 5.731

[4]. S. Ikram, J. Jacob, M. I. Arshad, K. Mahmood, A. Ali, N. Sabir, N. Amin, S. Hussain; Tailoring the structural, magnetic and dielectric properties of Ni-Zn $CdFe_2O_4$ spinel ferrites by the substitution of lanthanum ions; Ceram. Inter. 45 (2019) 3563-3569.

[5]. A. B. Kadam, V. K. Mande, S. B. Kadam, R. H. Kadam, S. E. Shirsath, R. B. Borade; Influence of gadolinium (Gd^{3+}) ion substitution on structural, magnetic and electrical properties of cobalt ferrites; J. Alloys. Comp. 840 (2020) 155669.

[6]. J. Hu, Y. Ma, X. Kan, C. Liu, X. Zhang, R. Rao, M. Wang, G. Zheng; Investigations of co-substitution on the structural and magnetic properties of Ni-Zn spinel ferrite; J. Magn. Magn. Mater. 513 (2020) 167200

[7]. V. D. More, S. S. Kadam, S. R. Kadam, S. R. Wadgane, R. H. Kadam, S. T. Alone; Complete micro-structural analysis and elastic properties of Sm^{3+} doped Ni-Mn-Zn mixed spinel ferrite nanoparticles; 400 (2021) 2100115.

[8]. M. Hashim, M. Raghasudha, S. S. Meena, J. Shah, S. E. Shirsath, S. Kumar, D. Ravinder, P. Bhatt, Alimuddin, R. Kumar, R. K. Kotnala; Influence of rare earth ion doping (De and Dy) on electrical and magnetic properties of cobalt ferrites; J. Magn. Magn. Mater. 449 (2018) 319-327.

[9]. V. Chaudhari, R. H. Kadam, M. L. Mane, S. E. Shirsath, A. B. Kadam, D. R. Mane; Effect of La^{3+} impurity on magnetic and electrical properties of Co-Cu-Cr-Fe nanoparticles; J. Nanosci. Nanotechn. 15 (2015) 4268-4275.

[10]. M. Houshiar, L. Jamilpanah; Effect of Cu dopant on the structural, magnetic and electrical properties of Ni-Zn ferrites; Mater. Res. Bull. 98 (2018) 213-218.

[11]. D. V. Phugate, R. B. Borade, S. B. Kadam, L. A. Dhale, R. H. Kadam, S. E. Shirsath, A. B. Kadam; Effect of Ho^{3+} ion doping on thermal, structural, and morphological properties of Co-Ni ferrite synthesized by sol-gel method; J. Supercond. Nov. Magn. 33 (2020) 3545-3554.

[12]. M. Yousuf, S. Nazir, M. Akbar, M. N. Akthar, A. Noor, E. Hu, M. A. K. Yousuf Shaikh, Y. Lu; Structural, magnetic and electrical evaluations of rare earth Gd^{3+} doped in mixed Co-Mn spinel ferrites; Ceram. Inter. 48 (2022) 578-586.

[13]. K. R. Desai, S. T. Alone, S. R. Wadgane, S. E. Shirsath, K. M. Batoo, A. Imran, E. H. Raslan, M. Hadi, M. F. Ijaz, R. H. Kadam; X-ray diffraction based Williamson-Hall analysis and Rietveld refinement for strain mechanism in Mg-Mn co-substituted $CdFe_2O_4$ nanoparticles; Physica B: Cond. Matter. 614 (2021) 413054.

[14]. Z. Karimi, Y. Mohammadifar, H. Shokrollahi, Sh. Khamenesh Asl., Gh. Yousefi, L. Karimi; Magnetic and structural properties of nano-sized Dy-doped cobalt ferrite synthesized by co-precipitation; J. Magn. Magn. Mater. 361 (2014) 150-156.

[15]. M. N. Akthar, M. A. Khan; Effect of rare earth doping on the structural and magnetic features of nanocrystalline spinel ferrites prepared via sol-gel route; J. Magn. Magn. Mater. 460 (2018) 268-277.

[16]. M. Hashim, A. Ahmed, S. A. Ali, S. E. Shirsath, M. M. Ismail, R. Kumar, S. Kumar, S. S. Meena, D. Ravinder; J. Alloys. Comp. 834 (2020) 155089.

[17]. M. M. Ismail, N. A. Jaber; Structural and elastic properties of nickel zinc ferrite nano-particles doped with lithium; J. Braz. Soc. Mech. Stud. Engg. 40 (2018) 250.

[18]. K. P. Thummer, A. R. Tanna, H. H. Joshi; Rietveld structure refinement and elastic properties of $MgAl_xCr_xFe_{2-2x}O_4$ spinel ferrites; AIP Conf. Proceedings 1837 (2017) 040058.

[19]. S. Debnath, K. Deb, B. Saha, R. Das; X-ray diffraction analysis for the determination of elastic properties of zinc doped manganese spinel ferrite nanocrystals ($Mn_{0.75}Zn_{0.25}Fe_2O_4$) along with the determination of ionic radii, bond lengths and hopping lengths; J. Phys. Chem. Solid. 134 (2019) 105-114.